`

# Aerodynamic parameters of flow around the cube in free stream using PIV

D. A. Dekterev [a,]*, P. A. Neobyavlyayuschiy [a]

[a] *Kutateladze Institute of Thermophysics of the Siberian Branch of the Russian Academy of Sciences, Novosibirsk, Russia*

**e-mail: dekterev_da@mail.ru*

**Abstract**

The paper presents experimental data of study flow around a cube mounted into aerodynamic tunnel. The cube's face height is 100 mm, and the cross-section of wind tunnel work section is 800 x 800 mm, it allows for a wall-free environment. The Reynolds number is Re = 50,000. Oil-film visualization and PIV were used to study the aerodynamics. Average velocity fields and velocity profiles in various cross-sections are presented. A database has been created for testing of CFD models.

## 1 Iintroduction

The evaluation of the current state of the ecological situation in modern cities indicates that unfavorable conditions often develop therein. The defining factor influencing the level of the ecological environment is the wind regime. The approaches used for planning residential microdistricts are primarily focused on social functionality (Antoniou et al. 2024) and they are almost not assessed from the perspective of territory aeration and wind comfort conditions.

Both computational methods and physical modeling in aerodynamic tunnels are used to study the aerodynamics of urban microdistricts (Blocken 2015).

Specialized software is being developed by specialists from the Siberian Federal University and the Institute of Thermophysics of the Siberian Branch of the Russian Academy of Sciences to research aeration regimes and ecological comfort in urban development conditions (Litvintsev et al. 2023). The correctness of computational fluid dynamics CFD modeling results directly depends on the proper resolution of large three-dimensional vortex structures formed in separation zones on building walls and roofs. As studies show, standard Reynolds-averaged Navier–Stokes (RANS) models do not fully resolve such problems, often significantly overestimating separation zones. In contrast, large eddy simulation (LES), when wind parameters are correctly specified, handles these problems better. However, LES requires significantly greater computational resources, making the modeling of large microdistricts or entire cities practically impossible. Therefore, there is a need to improve and tune RANS or hybrid models.

To do this, verification data are required, which was obtained through experiments with various building morphotypes in an aerodynamic tunnel using Oil-film visualization and particle image velocimetry (PIV).

The first task was to study the simplest object in the form of a cube. Classic experiments include works (Castro 1977) and (Martinuzzi and Tropea 1993). These describe characteristic flow structures formed around a cube. In the experiment Martinuzzi and Tropea (1993), a database was created using laser Doppler anemometry (LDA) for different sections around the cube. This data served for testing CFD models by various authors (Rodi 1996, Isaev and Lysenko 2009). However, the experiment is specific — the cube is placed in a working channel with a height of only 2H, where H is the height of the cube. This setup significantly differs from the flow around a cube in free space. The upstream flow profile in this work is fundamentally different from the logarithmic atmospheric profile.

In the literature, there are data on PIV (Ma et al. 2023, Khan et al. 2018) and even time-resolved PIV (Schröder et al. 2020), but despite the high interest in the aerodynamics of cubic bodies, no database of velocity fields and pulsation characteristics for flow around a cube in conditions close to unbounded in height and width has been found.

The task of conducting a systematic experimental study using field velocity measurement methods (PIV) to develop a verification database becomes critically important.

`

## 2 Experimental setup

### 2.1 Aerodynamic tunnel

The closed-type aerodynamic tunnel is shown in figure 1. The flow is generated by an axial fan with a capacity of 15 kW, operating in suction mode. The flow velocity in the working section varies from 0 to 20 m/s.

The working section has cross dimensions of 0.8 × 0.8 m and a length of 2.5 m, with optically transparent walls, allowing the application of optical flow measurement methods such as high-speed visualization, laser visualization, and PIV.

To create a uniform flow before the working section, a nozzle with a contraction cone is installed. Between the contraction and the turning section, there is a section containing the flow object, which disrupts the flow generated after the turning section.

The air temperature during the experiments can vary in the range of 20–25°C.

**Fig. 1** Aerodynamic tunnel

### 2.2 Aerodynamic model

Previously (Dekterev et al. 2023), studies were conducted on the influence of the scale factor on the aerodynamics of flow around a cubic body. Various aerodynamic facilities and research methods were used, as well as models with sizes ranging from 50 to 500 mm. Experiments, CFD simulations, and a review of literature data led to the conclusion that similar flow patterns are observed in the Reynolds number range from $Re = 2 \cdot 10^4$ to $4 \cdot 10^6$. This indicates the issue's similarity in different scales within the considered speed range. Differences in the boundaries of vortex zones in experimental works are presumably determined by the velocity profile of the approaching flow and, as analysis shows, by the level of turbulent pulsations of the incoming flow.

This work presents results for a thoroughly studied cube with a height H = 100 mm. Such a size allows for sufficiently detailed resolution of the flow structure around the cube. The flow velocity was set so that the Reynolds number, based on wind speed at height H, was Re = 50.000.

Figure 2 schematically illustrates the position of the cube relative to the axes of the adopted coordinate system and the approaching flow. The point "zero" corresponds to the front edge of the cube along the X-axis, the lower face of the cube along the Z-axis, and the central section (axis of symmetry) along the Y-axis.

`

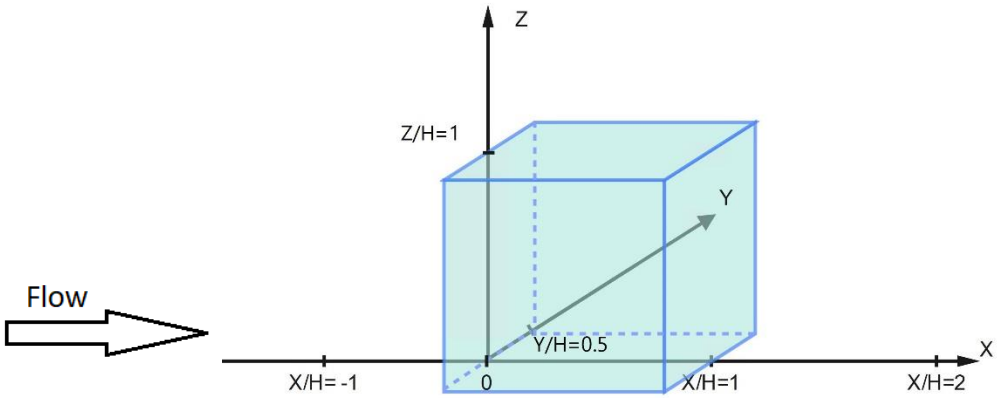


**Fig. 2** Coordinate system

Subsequently, the section coordinates are presented in relative values normalized by the height of the cube, H.

### 2.3 Oil-film visualization

To determine the boundaries of vortex zones on the underlying surface, the oil-film visualization method was used.

This method is considered traditional and has been employed in many studies (Martinuzzi and Tropea 1993, Meinders et al. 1999, Terekhov et al. 2010). In this work, kerosene with the addition of fine-dispersed pigment powder was used as the working fluid. The applicability of this approach is justified by earlier research.

The use of PIV in the ground boundary layer is hindered by surface over-illumination, while information on this zone is fundamentally important, especially when studying pedestrian comfort.

The images obtained from the oil-film experiment can serve as data for qualitative comparison with the surface stress fields obtained from CFD calculations.

Figure 3 shows an image obtained through the oil-film method for a cube with H = 100 mm and Re = 50.000.

**Fig. 3** Oil-film picture

### 2.4 PIV System

The PIV system consists of: a two-camera setup, featuring a 5 MPix ImperX IGV-B2520M-SC16 camera with a resolution of 2456 × 2058 pixels, equipped with a Nikon AF Nikkor 35mm 1:2D lens; a Beamtech Optronics Vlite-200 laser with a seven-joint fiber-optic delivery system for directing the laser beam into the experimental area and optical

`

attachments forming a laser sheet at various angles; a Polis synchronization processor; and specialized software for equipment synchronization, data collection, processing, and analysis in ActualFlow.

For tracers, micro-foamized $SiO_2$ particles ranging from 5 to 20 nm in size are introduced into the flow via a seeding device with compression equipment.

From the recorded tracer distributions in various experiments, background signals were subtracted as needed. These signals were calculated by averaging pixel brightness across all images in a series, to improve the signal-to-noise ratio.

Velocity fields were computed using an iterative cross-correlation algorithm with subpixel displacement and interrogation window deformation between iterations. The final interrogation window size was 16×16 pixels. The algorithm allows setting the overlap level between neighboring windows, which was fixed at 50%. It also accounts for the number of particles in each window: if fewer than five particles are detected, the velocity vector is not calculated in that region.

The measured area was approximately 220×180 mm. To study the flow in front of and behind the cube with H = 100 mm, imaging was performed in two sections with slight overlap.

A schematic layout of the frames in the XZ plane is shown in figure 4.

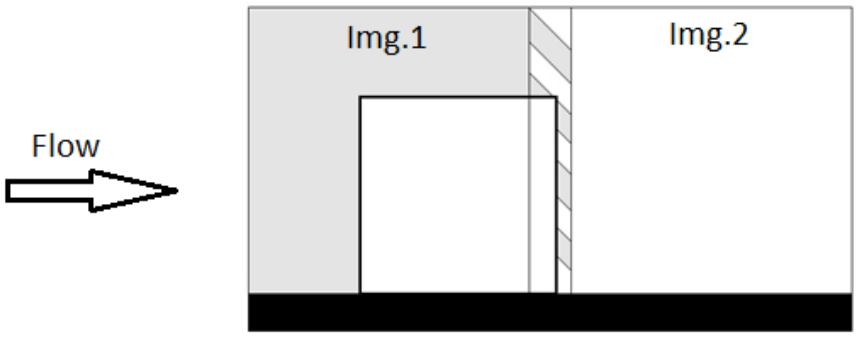


**Fig. 4** Position of frames in the XZ plane

When the camera was positioned from above (the XY plane), due to the symmetry of the flow around the cube, only one half of the cube was considered. This is schematically depicted in figure 5.

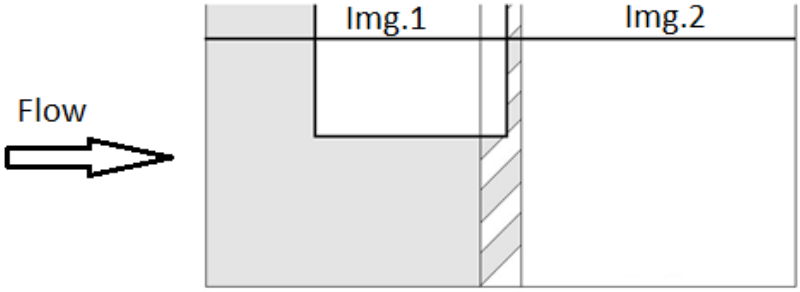


**Fig. 5** Position of frames in the XY plane

### 2.5 Parameters of the inlet flow

Preliminary studies of the velocity field formed in the working section of the aerodynamic tunnel, in the region where the cube is positioned, were conducted. For this, a PIV experiment was carried out without installing the aerodynamic model. To better resolve the turbulent characteristics of the flow, 1000 frames were recorded for subsequent processing and averaging of the data.

Below are the profiles of the X-component of velocity and the pulsation intensities Ix and Iz in the XZ section (side view) (Fig. 6), as well as the profile of the X-component of velocity and the pulsation intensities Ix and Iy in the XY section (top view) at height H (Fig. 7).

`

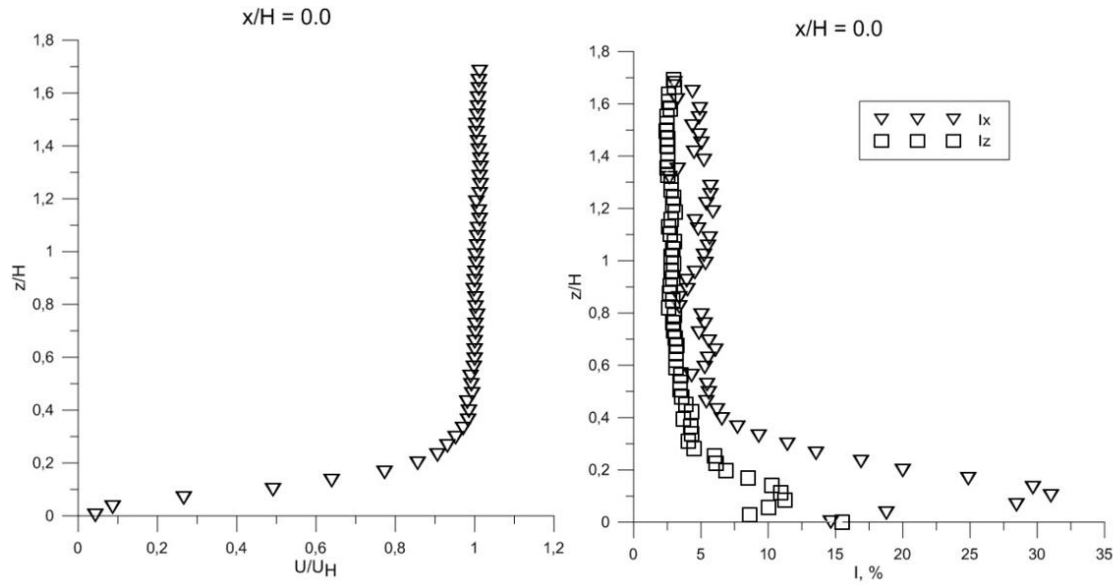


**Fig. 6** X-component velocity profile and XZ pulsation intensity

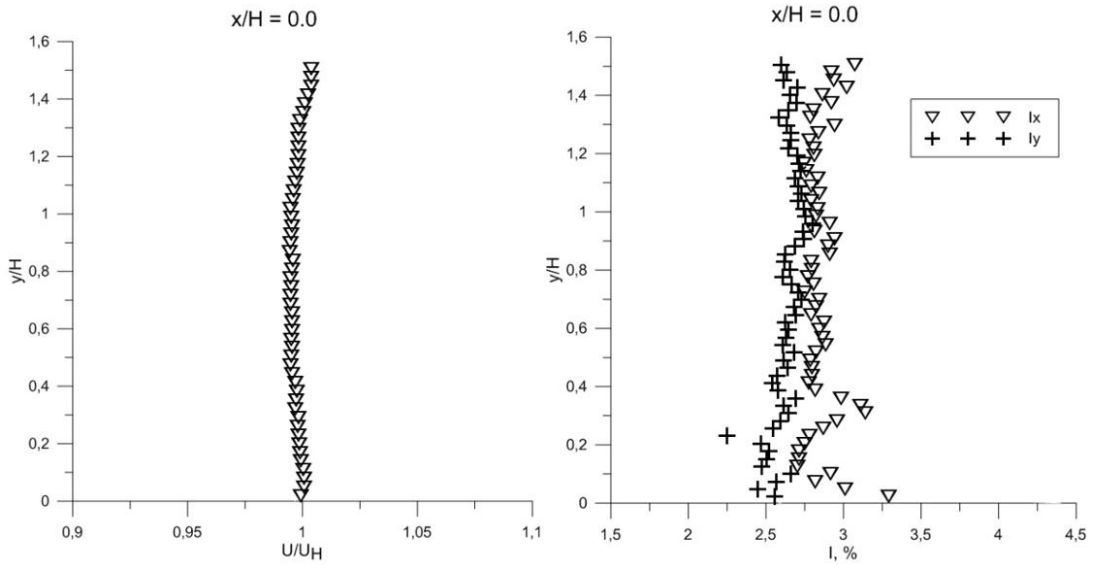


**Fig. 7** X-component velocity profile and XY pulsation intensity at height H

The boundary layer is estimated to be about 30–40 mm in height, so for a model with height H = 100 mm, most of it is in a uniform approaching flow with a low level of turbulent pulsations around I = 3–5%.

It is worth noting that the pulsation intensity in the velocity of the real atmospheric wind flow ranges between 10–20%.

### 3 Results and discussion

A cube model was installed in the working section of the wind tunnel, and a series of experiments were conducted.

From a side view (XZ plane), three cross-sections along the depth were studied: Y/H=0 – the center of the cube, Y/H=0.25, and Y/H=0.5 – the side wall of the cube.

Figures 8-10 show the averaged vector fields of the X-component of velocity in these cross-sections.

`

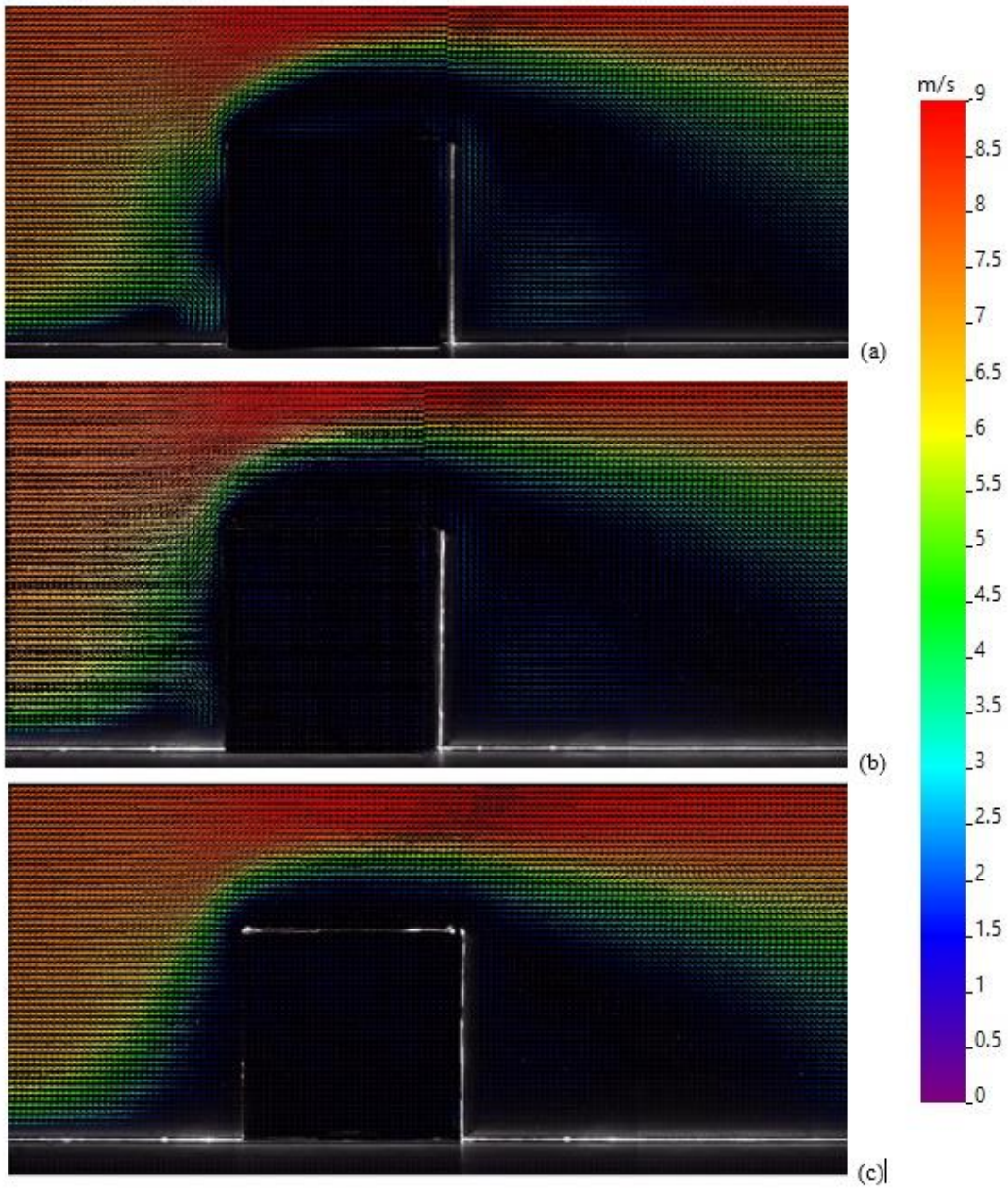


**Fig. 8** Flow patterns in sections (a) Y/H = 0.5, (b) Y/H = 0.25, (c) Y/H = 0.0

The profiles of the X-component of velocity in these planes for different cross-sections along the length (X/H) are shown in figure 9.

`

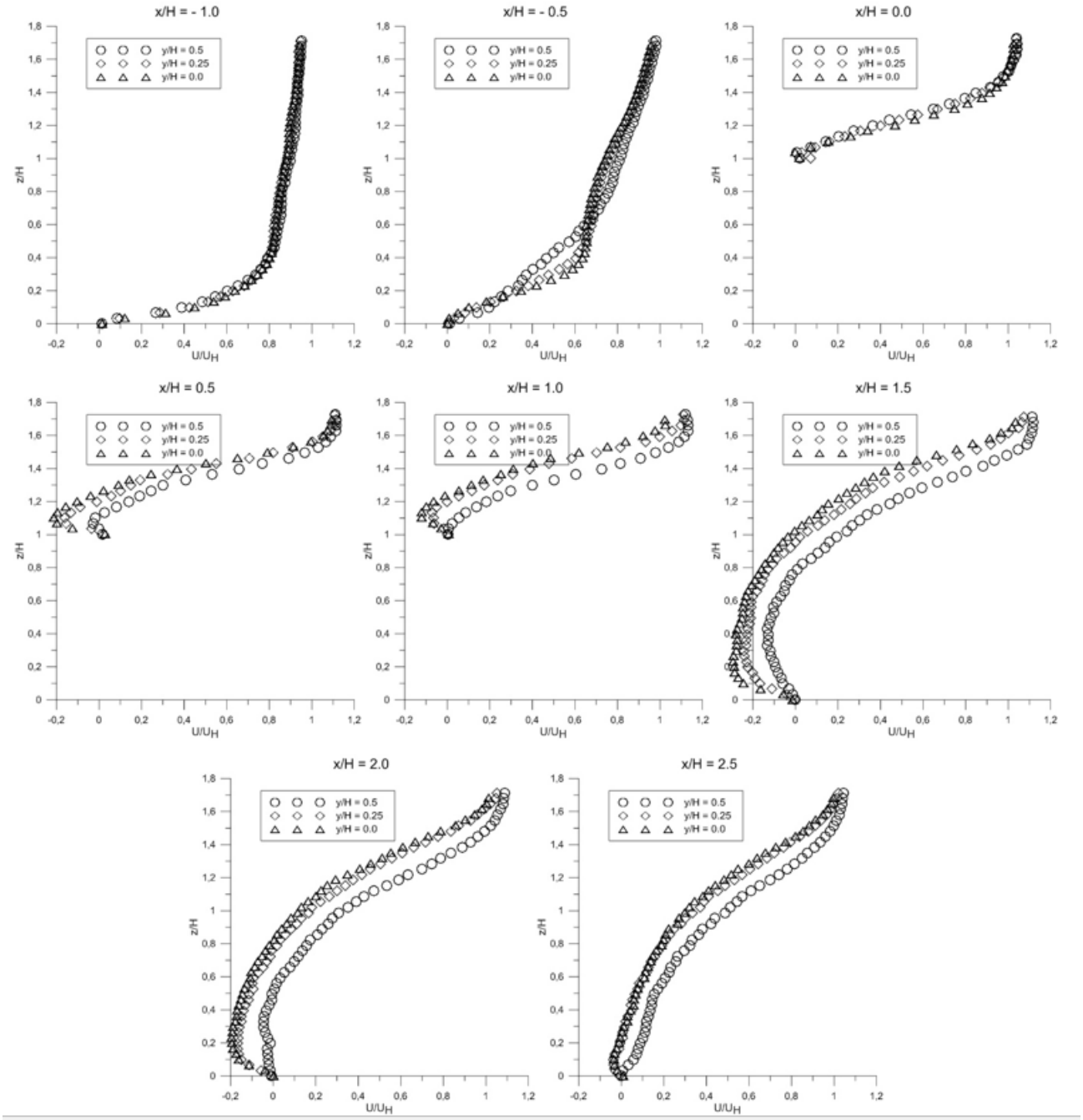


**Fig. 9** X-component velocity profiles for sections Y/H=0.5, 0.25, 0 and various distances relative to the X/H cube

For a top view (XY plane), seven cross-sections along the height were constructed, corresponding to Z/H=0.25, 0.5, 0.75, 1, 1.1, 1.2, and 1.3.

Flow patterns at Z/H=0.25, 0.5, and 1 are shown in figure 10.

`

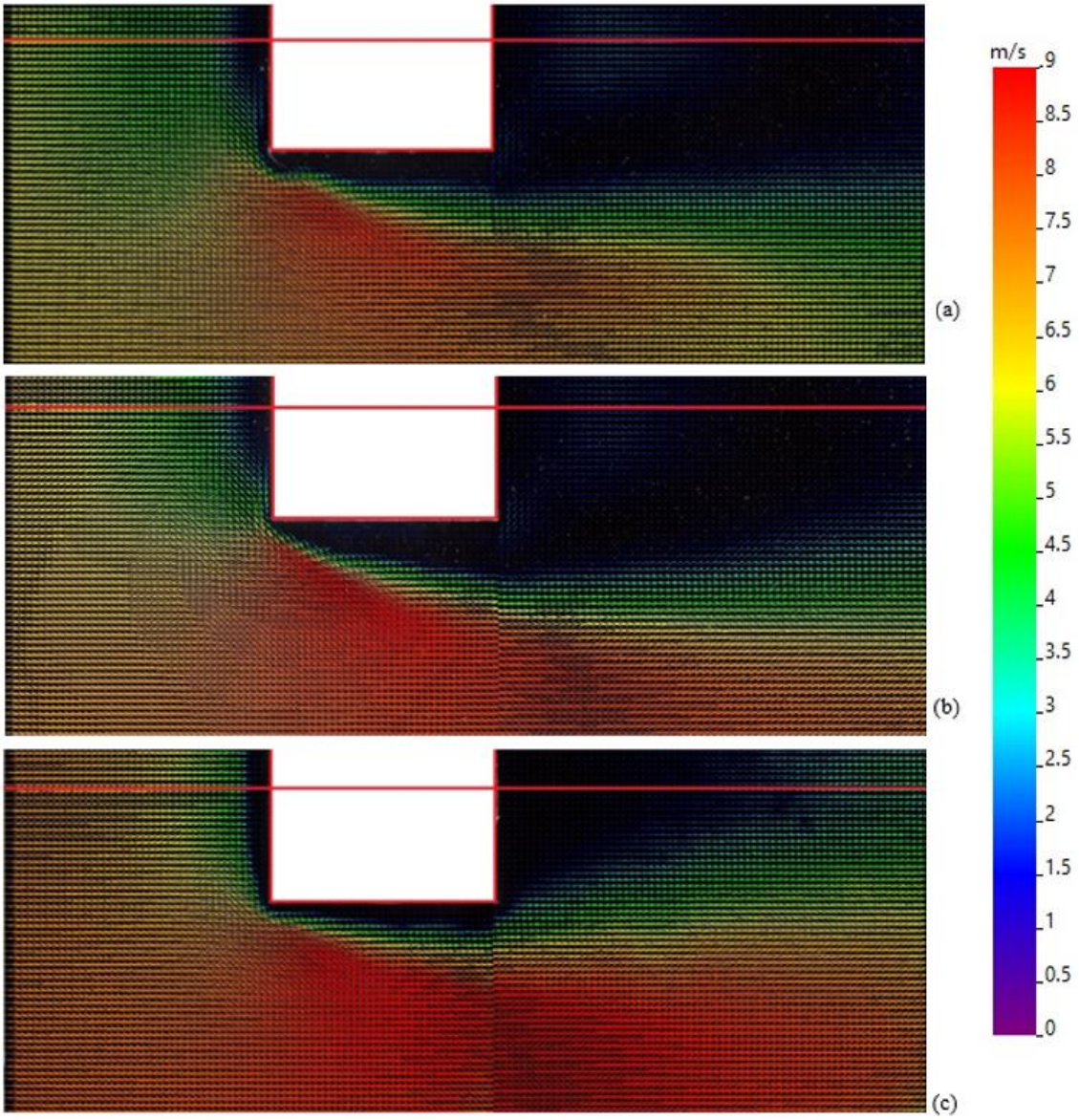


**Fig. 10** Flow patterns in sections Z/H=0.25, 0.5, 1

The profiles of the X-component of velocity in these planes for different cross-sections along the length (X/H) are shown in figure 11.

`

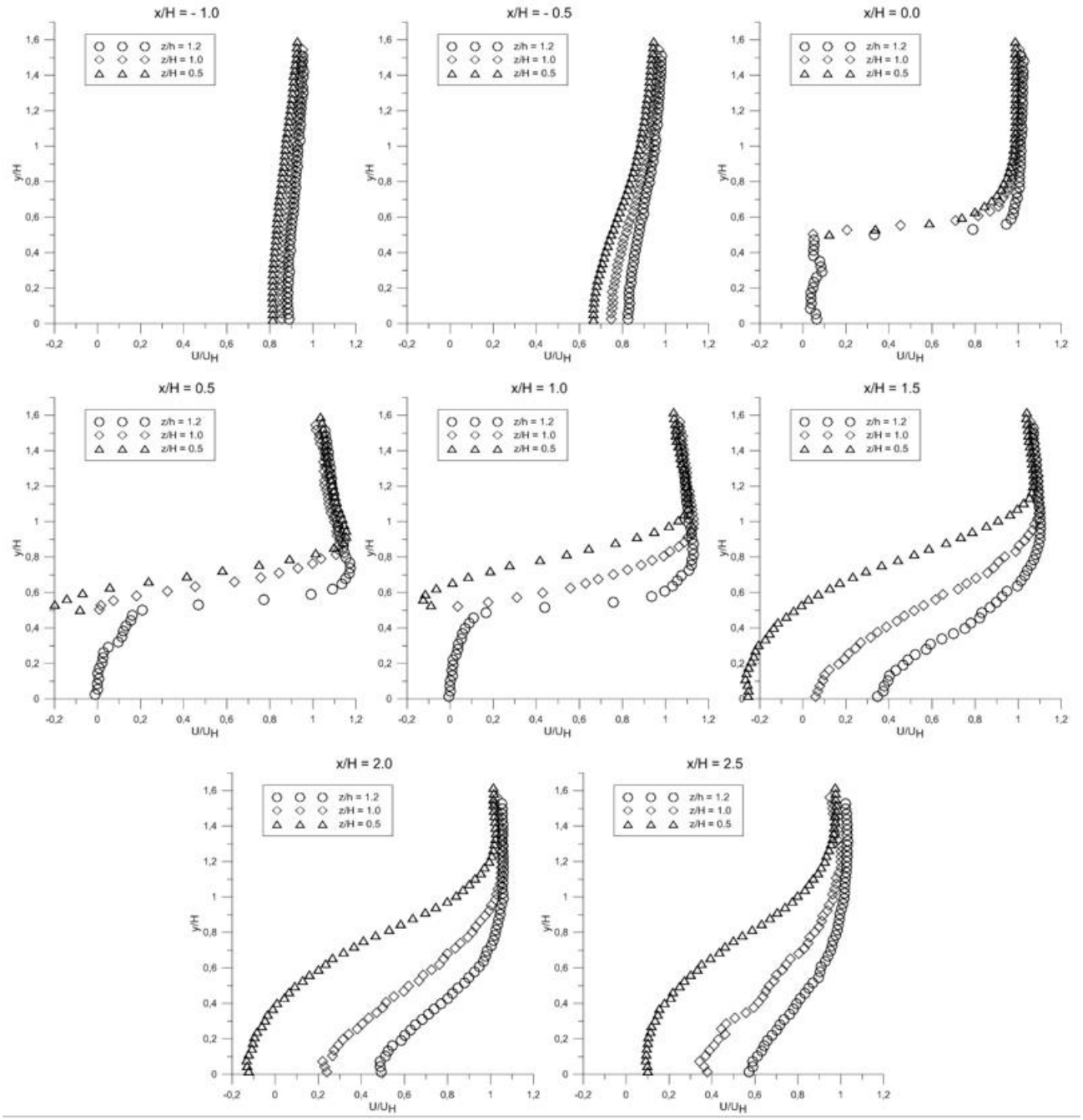


**Fig. 11** Flow patterns in sections Z/H=0.5, 1, 1.2

As an example, a comparison is made with the profiles of Martinuzzi (1993), demonstrating the influence of a closely located upper wall on the flow near a cube.

`

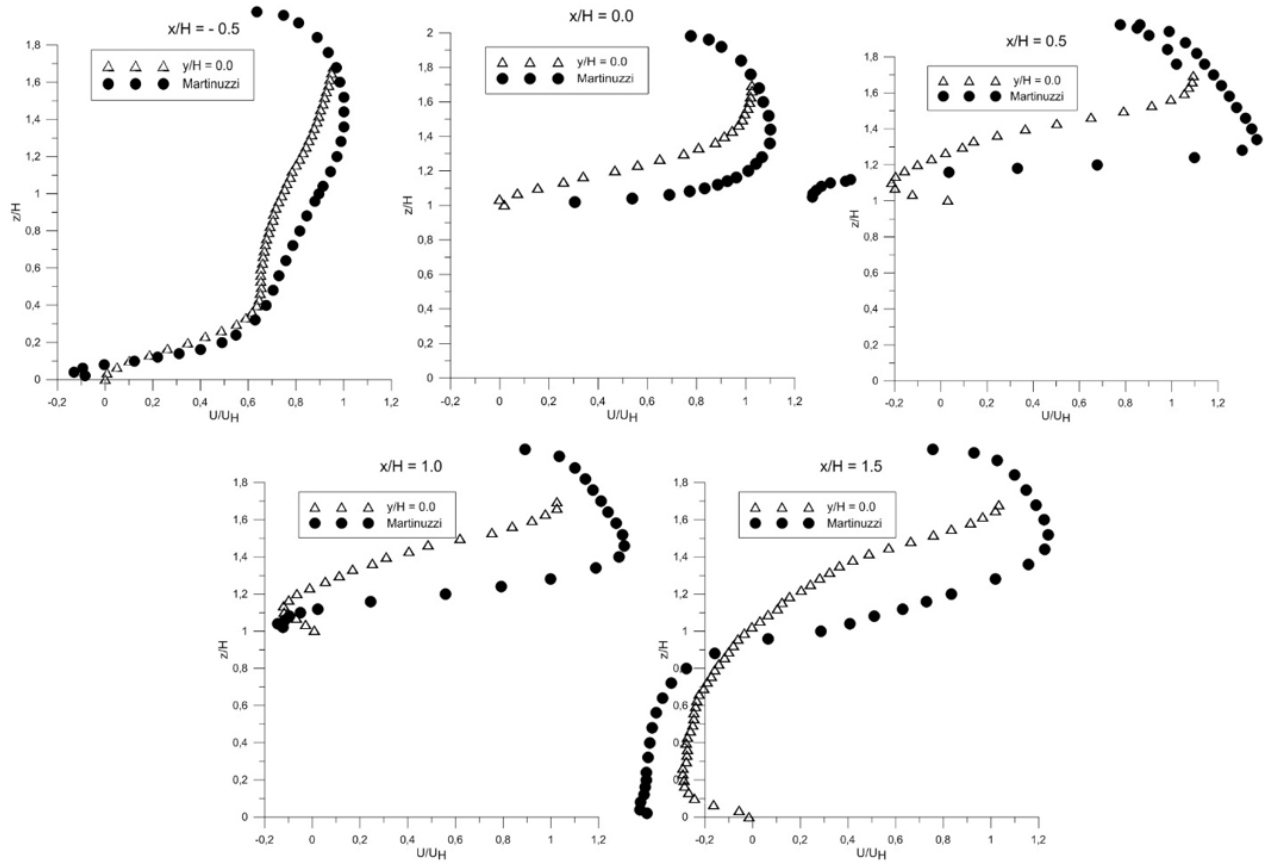


**Fig. 12** Comparison of data with Martinuzzi (1993)

From the graphs, it is evident that in the Martinuzzi (1993) case, an accelerated flow develops above the surface of the cube, with velocity values exceeding $U/U_H = 1$ at the cross-section X/H = -0.5. In our case, however, all velocity values at that cross-section are less than $U/U_H = 1$.

## 4 Conclusions

In this paper, most of the presented data pertains to the X-component of velocity (as the most indicative) during the flow around a cube in free space, for selected cross-sections in the XZ and XY planes. Based on the results of the study, a database of 2D velocity fields and their fluctuations in various cross-sections has been developed. Such data are of great interest for use as a verification base for calibrating and testing CFD models (RANS, LES, and hybrid approaches). In particular, they will facilitate the tuning and validation of numerical methods for developing software tools to study aeration regimes and environmental comfort in urban areas.

## Declarations

Funding

The study was supported by the Russian Science Foundation (Grant No. 22-61-00098), https://rscf.ru/project/22-61-00098/

Competing of interest

The authors have no competing interests to declare that are relevant to the content of this article.

`

REFERENCES


Antoniou N., Montazeri H., Blocken B., Neophytou M. (2024) On the impact of climate change on urban microclimate, thermal comfort, and human health: Multiscale numerical simulations. Build. Environ. V. 60. P. 111690. https://doi.org/10.1016/j.buildenv.2024.111690

Blocken B. (2015) Computational Fluid Dynamics for urban physics: Importance, scales, possibilities, limitations and ten tips and tricks towards accurate and reliable simulations. Build. Environ. V. 91. P. 219. http://dx.doi.org/10.1016/j.buildenv.2015.02.015

Castro I. and Robins A. (1977) The flow around a surface-mounted cube in uniform and turbulent streams. J. Fluid Mech., Vol. 79, P. 307–335. https://doi.org/10.1017/S0022112077000172

Dekterev, D. A., Lobasov, A. S., Meshkova, V. D., Litvintsev, K. Y., Dekterev, A. A., & Dekterev, A. A. (2023). The influence of scale factor on simulation results for flow around buildings. Thermophysics and Aeromechanics, 30(6), 1131-1137. https://doi.org/10.1134/S086986432306015X

Isaev S.A., Lysenko D.A. (2009.) Calculation of unsteady flow around a cube on the wall of a narrow channel using URANS and the Spalart–Allmares turbulence model. IFZ. Vol. 82. № 3. P. 429.

Khan, M. H., Sooraj, P., Sharma, A., & Agrawal, A. (2018). Flow around a cube for Reynolds numbers between 500 and 55,000. Experimental thermal and fluid science, 93, 257-271. https://doi.org/10.1016/j.expthermflusci.2017.12.013

Litvintsev, K. Y., Dekterev, A. A., Meshkova, V. D., & Filimonov, S. A. (2023). Influence of radiation on the formation of wind and temperature regimes in urban environment. Thermophysics and Aeromechanics, 30(4), 683-694. https://doi.org/10.1134/S086986432304008X

Ma, L., Kashanj, S., Li, X., Xu, S., Nobes, D. S., & Ye, M. (2023). Experimental investigation of fluid flow around a porous cube for Reynolds numbers of 400–1400. Chemical Engineering Science, 269, 118443. https://doi.org/10.1016/j.ces.2022.118443

Martinuzzi R. and Tropea C., (1993) The flow around surface-mounted, prismatic obstacles placed in a fully developed channel flow (data bank contribution), J. Fluids Engng.Vol. 115, Iss. 1, P. 85–92. https://doi.org/10.1115/1.2910118

Meinders, E. R., Hanjalic, K., & Martinuzzi, R. J. (1999). Experimental study of the local convection heat transfer from a wall-mounted cube in turbulent channel flow. Journal of heat transfer, 121(3), 564-573. https://doi.org/10.1115/1.2826017

Rodi W. (1997) Comparison of LES and RANS calculations of the flow around bluff bodies, J. Wind Engng Industrial Aerodynamics, Vol. 69, P. 55–75. https://doi.org/10.1016/S0167-6105(97)00147-5

Schröder, A., Willert, C., Schanz, D., Geisler, R., Jahn, T., Gallas, Q., & Leclaire, B. (2020). The flow around a surface mounted cube: a characterization by time-resolved PIV, 3D Shake-The-Box and LBM simulation. Experiments in Fluids, 61(9), 189. https://doi.org/10.1007/s00348-020-03014-5

Terekhov V.I., Gnyrya A.I. and Koroibkov S.V. (2010) Vortex pattern of the turbulent flow around a single cube on a flat surface and its heat transfer at different attack angles, Thermophysics and Aeromechanics,Vol. 17, No. 4, P. 489–500. https://doi.org/10.1134/S0869864310040037